Proceedings of the 8th International Conference on Structural Dynamics, EURODYN 2011
Leuven, Belgium, 4-6 July 2011
G. De Roeck, G. Degrande, G. Lombaert, G. Müller (eds.)
ISBN 978-90-760-1931-4

Experimental Model-Reference Composite Control of Lightweight Flexible Manipulators

Ayman A. El-Badawy [1], Amir R. Ali [2]
[1] Mechanical Engineering Department, Al-Azhar University, Cairo, Egypt
[2] Department of Mechatronics Engineering, The German University in Cairo, Cairo, Egypt
email: ayman.elbadawy@guc.edu.eg, amir.ali@guc.edu.eg

ABSTRACT: In this paper, a composite control, based on singular perturbation formulation, is utilized to suppress the oscillations of a flexible-link manipulator and to enable better tip positioning as it follows a desired trajectory. The control strategy is then implemented on two different hardware architectures. The first architecture uses a data-acquisition card and a personal computer (DAQ system). The second architecture uses a programmable automation controller (PAC) which uses field-programmable gate array technology. A model-reference control strategy is developed and implemented in the case of a DAQ system to enhance this architecture performance by improving the dynamic behavior of the system. The system response using DAQ with a model-reference control algorithm is then compared with that using PAC.

KEY WORDS: Model-reference; Flexible manipulator; Composite control.

1 INTRODUCTION

Dynamics and control of multi-link flexible manipulators, unlike the general structure vibration and its control, are complicated due to the strong coupling between the nonlinear rigid body motions and the elastic deformation of the links during large motions of the manipulator. The challenges are associated with problems in dealing with the nonlinearities and uncertainties, such as the fact that the system inertia and the mode shapes vary with the configuration of the system, the flexible variables have no direct control inputs and the inverse dynamics and inverse kinematics problems are coupled [1, 2].
The challenge of controlling vibrations in flexible structures, such as robotic manipulators, has been approached with very different methods, from classical schemes [3-5], linear quadratic regulator (LQR) control and feedback linearization control [6], to nonlinear methods such as sliding control [7]. Neural network based controller [8], adaptive control, and optimal control techniques was also formulated and implemented [9-11]. Variable structure control method in the control of a one-link flexible manipulator moving in horizontal plane was also used [12-14]. A composite control, based on singular perturbation formulation was also used for the same problem [15]. In this scheme, a slow control is designed for the slow subsystem, which is shown to be the model of the equivalent rigid-link manipulator. Then a fast control is designed to stabilize the fast subsystem which represents the vibration around the equilibrium trajectory setup by the slow subsystem under the effect of the slow control. This form enables improved control technique to be devised so that performance can be optimized [16]. The singular perturbation approach gives better performance and greater simplicity when compared with various control schemes for a single flexible robot arm, since it requires a limited amount of actuators [17]. A recent survey gives a complete, detailed overview of all the work developed in this field since the late 1970s [18].

The effect of the hardware used on the implementation of the developed control algorithm is in fact an important factor to the overall success of the control system. In this paper, the singular perturbation form of the dynamic equations of the robot manipulator is provided to derive a composite control. An experimental study is then implemented which requires timely decisions to be made based on incoming data on two different hardware architectures, namely data-acquisition card with a personal computer (DAQ system) and programmable automation controller (PAC) which uses field-programmable gate array technology. The first architecture is combined with a model-reference control strategy to improve the dynamic behavior of the motor for the position control of a one-link flexible arm. It is shown that the feedback control using the model-reference may be enough to shift the end position to the desired position provided that accurate synchronization between the incoming sensor signal and control signal is achieved. The output response is then compared with a PAC system which combines the flexibility of a FPGA with the reliability of a real-time processor.

2 DYNAMICS OF FLEXIBLE-LINK MANIPULATOR

Figure 1 presents the structure of the flexible manipulator considered in this study, which consists of one flexible arm. The arm is actuated at the joint by one motor. The manipulator is assumed to move in the horizontal plane; the gravitational effects of the manipulator system are therefore ignored. X_0Y_0 is the inertial frame; XY is the moving frame associated with the link.

An inertial payload of mass M_P and inertia J_p is connected at the end of the link. The effects of rotary inertia and shear deformation are ignored by assuming that the cross-sectional area of the link is small in comparison to the length L. The bending deflection $u(\eta,t)$ at a point η on the link can be

expressed as in equation (1) using the assumed-mode approach as a superposition of its natural modes of vibration.

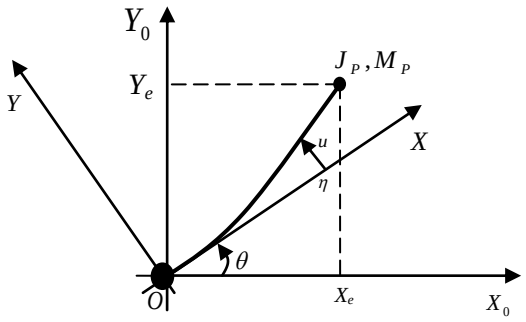

Figure 1. Structure of the flexible one-link manipulator

$$u(\eta,t)=\sum_{j=1}^{m}\delta_j(t)\phi_j(\eta) \tag{1}$$

where ϕ_j is the mode shape function [19], δ_j is the time-varying modal displacement and m is the number of finite modes. Two modes of vibrations are considered to describe the deflection of the link, as higher modes are considered to be very small and therefore negligible.

After some algebraic manipulations based on the Lagrangian-Euler assumed modes method [19], the final dynamic equations of motion of the manipulator can be written in compact form as in the following equations:

$$\begin{bmatrix}\mathbf{M}_{11} & \mathbf{M}_{12} & \mathbf{M}_{13}\\ \mathbf{M}_{21} & \mathbf{M}_{22} & \mathbf{M}_{23}\\ \mathbf{M}_{31} & \mathbf{M}_{32} & \mathbf{M}_{33}\end{bmatrix}\begin{bmatrix}\ddot{\boldsymbol{\theta}}\\ \ddot{\boldsymbol{\delta}}_1\\ \ddot{\boldsymbol{\delta}}_2\end{bmatrix}+\begin{bmatrix}\mathbf{g}_1(q,\dot{q},\delta,\dot{\delta})\\ \mathbf{g}_{21}(q,\dot{q},\delta,\dot{\delta})\\ \mathbf{g}_{22}(q,\dot{q},\delta,\dot{\delta})\end{bmatrix}+\begin{bmatrix}0 & 0\\ \mathbf{k}_{1e} & 0\\ 0 & \mathbf{k}_{2e}\end{bmatrix}\begin{bmatrix}\boldsymbol{\delta}_1\\ \boldsymbol{\delta}_2\end{bmatrix}=\begin{bmatrix}\mathbf{U}\\ 0\\ 0\end{bmatrix} \tag{2}$$

where $\mathbf{M}$ is the mass matrix, $\mathbf{k}$ is the stiffness matrix due to the distributed flexibility of the link, $\boldsymbol{\delta}$ is the modal displacement vector, $\boldsymbol{\theta}$ is the rotor angle vector, $\mathbf{U}$ is the actuator torque $\mathbf{g}_1$ and $\mathbf{g}_2$ are vectors containing terms due to interactions of the link angles and their rates with the modal displacement and their rates. M, g and K are in Appendix A

3 TWO-TIME-SCALE SINGULAR PERTURBATION MODEL OF THE FLEXIBLE-LINK-MANIPULATOR

Flexible link robots inherently contain both slow and fast dynamical phenomena, thus, they can be divided into two-time-scale sub-systems by using a small singular perturbation parameter ε, which is a small positive scalar dimensionless parameter. This is determined from the physical properties of the system to deal with its two-time-scale behavior. In the present case of the flexible link manipulator, ε is extracted from the flexural spring constant $\mathbf{k}$ of the link, which is discussed later in this section. The dynamic model of the manipulator with flexible link obtained in Eq.(2) is transformed into two-time-scale singular perturbation model as follows. The inertia matrix $\mathbf{M}$ is positive definite matrix, its inverse matrix, $\mathbf{H}$ can thus put in the following form:

$$\mathbf{M}^{-1}=\mathbf{H}=\begin{bmatrix}\mathbf{H}_{11[n\times n]} & \mathbf{H}_{12[n\times m]}\\ \mathbf{H}_{21[m\times n]} & \mathbf{H}_{22[m\times m]}\end{bmatrix} \tag{3}$$

where **n** is the number of the joints. Hence, using the above partitioned matrix in equation (2), $\ddot{\mathbf{q}}$ and $\ddot{\boldsymbol{\delta}}$ can be determined as follows:

$$\ddot{\mathbf{q}}=-\mathbf{H}_{11}(q,\mu\zeta)\mathbf{g}_1(q,\dot{q},\mu\zeta,\mu\dot{\zeta})-\mathbf{H}_{12}(q,\mu\zeta)\mathbf{g}_2(q,\dot{q},\mu\zeta,\mu\dot{\zeta})-\mathbf{H}_{12}(q,\mu\zeta)\zeta+\mathbf{H}_{11}(q,\mu\zeta)\mathbf{u} \tag{4.a}$$

$$\mu\ddot{\zeta}=-\mathbf{H}_{21}(q,\mu\zeta)\mathbf{g}_1(q,\dot{q},\mu\zeta,\mu\dot{\zeta})-\mathbf{H}_{22}(q,\mu\zeta)\mathbf{g}_2(q,\dot{q},\mu\zeta,\mu\dot{\zeta})-\mathbf{H}_{22}(q,\mu\zeta)\zeta+\mathbf{H}_{21}(q,\mu\zeta)\mathbf{u} \tag{4.b}$$

Now, define a common scale factor k_c, which is the minimum of all the stiffness constants, i.e. k_c= min (k_1, k_2, … , k_n) with this common scale factor, the flexural spring constant $\mathbf{k_i}$ can be scaled by k_c such that $\tilde{\mathbf{k}}_\mathbf{i}=(1/k_c)\mathbf{k}_\mathbf{i}$ and $\mu=1/k_c$.

To obtain the slow and the fast subsystems for the singular perturbation model of the flexible link manipulator μ is set to zero in the above Eq. (4). Solving for $\bar{\zeta}$ then yields (using the 'overbar' to indicate the value of the variable at $\mu=0$).

$$\bar{\zeta}=\mathbf{H}_{22}^{-1}(\bar{q},0)[-\mathbf{H}_{21}(\bar{q},0)\mathbf{g}_1(\bar{q},\dot{\bar{q}},0,0)+\mathbf{H}_{21}(\bar{q},0)\bar{\mathbf{u}}]-\mathbf{g}_2(\bar{q},\dot{\bar{q}},0,0) \tag{5}$$

The next step is to convert the singular perturbation model of the flexible link given though equations (4.a) and (4.b) into the state-space form. For this, the following state variables are chosen:

$$\mathbf{x}_1=\mathbf{q},\qquad \mathbf{x}_2=\dot{\mathbf{q}},\qquad \mathbf{z}_1=\zeta,\qquad \mathbf{z}_2=\varepsilon\dot{\zeta}$$

where $\varepsilon=\sqrt{\mu}$ then, using the above state variables in Eq.(4), the following state-space representation of the singular perturbation model is obtained:

$$\begin{aligned}\dot{\mathbf{x}}_1&=\mathbf{x}_2,\\ \dot{\mathbf{x}}_2&=-\mathbf{H}_{11}(x_1,\varepsilon^2z_1)\mathbf{g}_1(x_1,x_2,\varepsilon^2z_1,\varepsilon z_2)-\mathbf{H}_{12}(x_1,\varepsilon^2z_1)\mathbf{g}_2(x_1,x_2,\varepsilon^2z_1,\varepsilon z_2)\\ &\quad-\mathbf{H}_{12}(x_1,\varepsilon^2z_1)\mathbf{z}_1+\mathbf{H}_{11}(x_1,\varepsilon^2z_1)\mathbf{u}\end{aligned} \tag{6.a}$$

$$\begin{aligned}\varepsilon\dot{\mathbf{z}}_1&=\mathbf{z}_2,\\ \varepsilon\dot{\mathbf{z}}_2&=-\mathbf{H}_{21}(x_1,\varepsilon^2z_1)\mathbf{g}_1(x_1,x_2,\varepsilon^2z_1,\varepsilon z_2)\\ &\quad-\mathbf{H}_{22}(x_1,\varepsilon^2z_1)\mathbf{g}_2(x_1,x_2,\varepsilon^2z_1,\varepsilon z_2)-\mathbf{H}_{22}(x_1,\varepsilon^2z_1)\mathbf{z}_1\\ &\quad+\mathbf{H}_{21}(x_1,\varepsilon^2z_1)\mathbf{u}\end{aligned} \tag{6.b}$$

To obtain the slow subsystem, it is necessary to set $\varepsilon = 0$ in Eq.(6), which results in the following equations:

$$\dot{\bar{\mathbf{x}}}_1 = \bar{\mathbf{x}}_2, \qquad \dot{\bar{\mathbf{x}}}_2 = \mathbf{M}_{11}^{-1}(\bar{x}_1) \times [\bar{\mathbf{u}}] \tag{7}$$

It can be seen that Eq.(7) is the state-space model of the rigid link manipulator.

To obtain the fast subsystem, a fast time-scale defined by $\tau = t/\varepsilon$ is introduced. It may be noted that, at ($\varepsilon = 0$), $dx_1/d\tau$ and $dx_2/d\tau$, g_1 and g_2 are zero. Hence in the fast time-scale, defining new fast variables as:

$$\boldsymbol{\eta}_1 = \mathbf{z}_1 - \bar{\boldsymbol{\zeta}}, \qquad \boldsymbol{\eta}_2 = \mathbf{z}_2 \tag{8}$$

and with substitution of these fast variables corresponding to the state variables z_1 and z_2 in Eq.(6), the fast subsystem can be written in state variable form as follows:

$$\dot{\mathbf{x}}_\mathbf{f} = \mathbf{A}_\mathbf{f}\mathbf{x}_\mathbf{f} + \mathbf{B}_\mathbf{f}\mathbf{u}_\mathbf{f} \tag{9}$$

with $\mathbf{A}_\mathbf{f} = \begin{bmatrix} \mathbf{0} & \mathbf{I} \\ -\mathbf{H}_{22} & \mathbf{0} \end{bmatrix}$, $\mathbf{B}_\mathbf{f} = \begin{bmatrix} \mathbf{0} \\ \mathbf{H}_{21} \end{bmatrix}$, and $\mathbf{x}_\mathbf{f} = [\boldsymbol{\eta}_1 \quad \boldsymbol{\eta}_2]$

where the **0** and **I** are matrices of appropriate dimensions.

4 DESIGN OF SINGULAR PERTURBATION CONTROL SCHEME

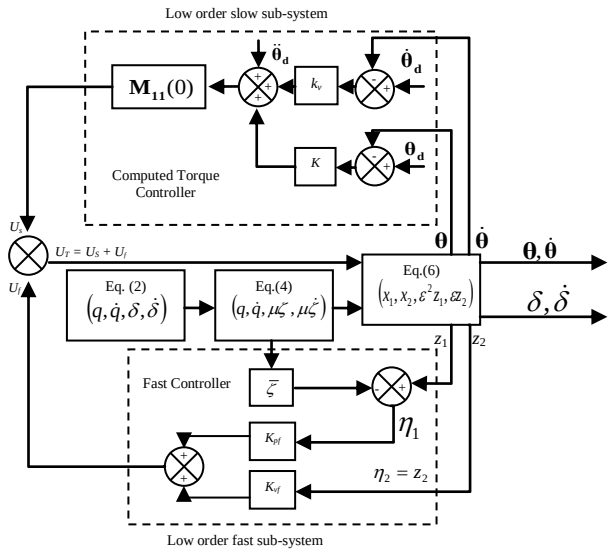

Figure 2. Singular perturbation control scheme

Figure 2 shows the structure for the singular perturbation controller. On the basis of the two-time-scale model for the manipulator with single-link flexible manipulator given in Eq.(7) and (9), the design of feedback controller for the system can be performed according to a composite strategy [20].

$$\mathbf{u} = \bar{\mathbf{u}}(\bar{\mathbf{x}}_1, \bar{\mathbf{x}}_2) + \mathbf{u}_\mathbf{f}(\bar{\mathbf{x}}_1, \boldsymbol{\eta}_1, \boldsymbol{\eta}_2) \tag{10}$$

where $\bar{\mathbf{u}}$ and $\mathbf{u}_\mathbf{f}$ are the slow and fast control signals respectively.

The controller for the slow subsystem can be designed according to the well-known computed torque control technique used for rigid manipulators, which can be written as:

$$\bar{\mathbf{u}} = \mathbf{M}_{11}(\mathbf{0})[\ddot{\boldsymbol{\theta}}_\mathbf{d} + \mathbf{k}_\mathbf{v}(\dot{\boldsymbol{\theta}}_\mathbf{d} - \dot{\boldsymbol{\theta}}) + \mathbf{k}_\mathbf{p}(\boldsymbol{\theta}_\mathbf{d} - \boldsymbol{\theta})] \tag{11}$$

where $\mathbf{k}_\mathbf{v}$ and $\mathbf{k}_\mathbf{p}$ are the diagonal velocity and position gain matrices of the controller respectively and $\boldsymbol{\theta}_\mathbf{d}$, $\dot{\boldsymbol{\theta}}_\mathbf{d}$ and $\ddot{\boldsymbol{\theta}}_\mathbf{d}$ are the desired trajectory position, velocity, and acceleration of the link respectively.

Because the pair ($\mathbf{A_f}$, $\mathbf{B_f}$) of the fast subsystem in Eq.(9) are completely state controllable, a state feedback control can be devised to force its states $\mathbf{x_f}$ to zero, as given below:

$$\mathbf{u}_\mathbf{f} = \mathbf{k}_\mathbf{pf}\, x_f + \mathbf{k}_\mathbf{vf}\, \frac{dx_f}{d\tau} \tag{12}$$

Where the feedback gains $\mathbf{k_{pf}}$ and $\mathbf{k_{vf}}$ are obtained through optimizing the cost function using an LQR technique [21].

5 SIMULATION RESULTS

The non-linear differential equation (Eq. 2) was simulated using a fourth-order Runge-Kutta [22] integration method. The flexible arm is constructed using a piece of thin stainless-steel with length L=0.3 m, mass m=0.2 kg, cross-sectional area A=1.692 mm^2, flexural rigidity EI=40 N.m^2, mass density per unit volume ρ=8190 kg/m^3, joint inertia I_0=0.337 kg.m^2, link inertia relative to joint J_0=0.0369 kg.m^2, payload mass M_p=0.25 kg and payload inertia J_p=0.0065 kg.m^2; these values are obtained from the experiment.

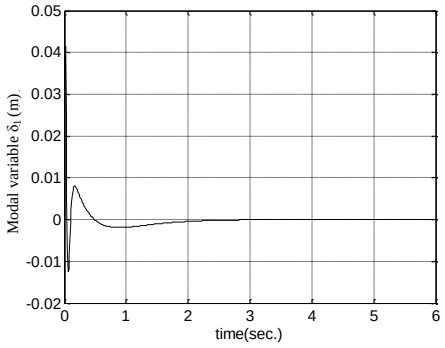

Figure 3a. First modal variable δ_1

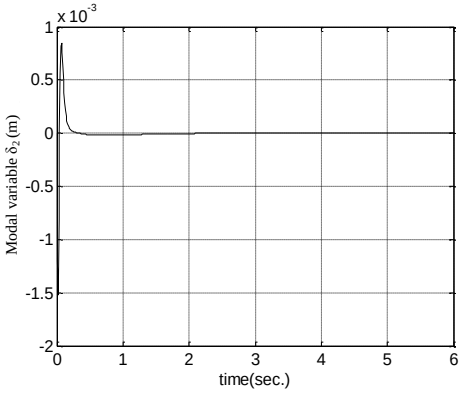

Figure 3b. Second modal variable δ_2

It can be shown from Figures 3a, 3b that the control of the first and second modes of the link vibrations has been damped at steady state in less than one second while the motor has reached its desired trajectory as shown in Figures 3c, 3d.

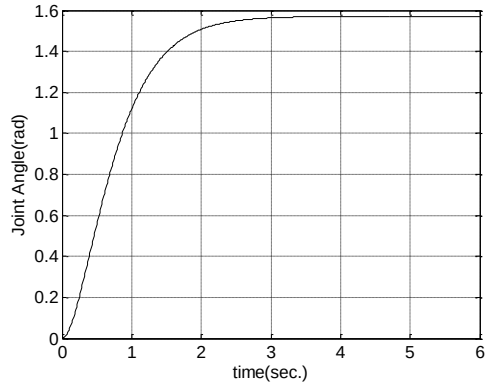

Figure 3c. Joint angle

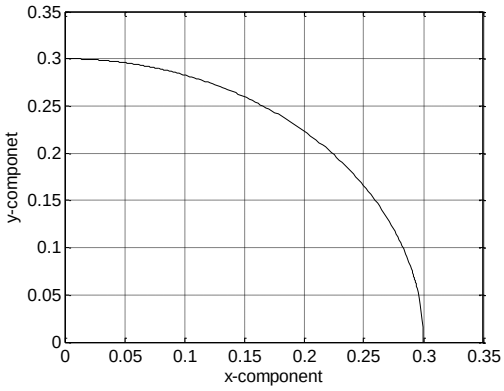

Figure 3d. End-Effector in space

The design of a feedback control for the full system Eq. (6) is shown in Figure 3e which can be split into slow control $\bar{\mathbf{u}}$ and fast control $\mathbf{u_f}$ as shown in Figures (3f, 3g). From these two figures, it is clear that the two control signals are of comparable magnitude. Hence, the fast control signal adjusts the slow control signal so as to minimize the link oscillations while still following the desired trajectory.

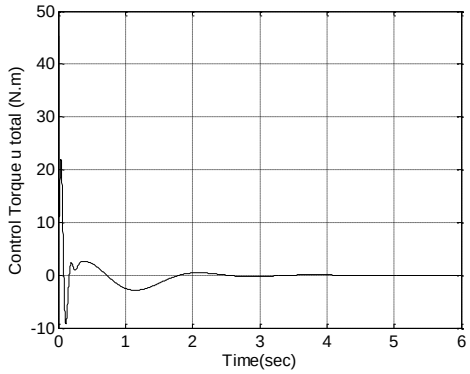

Figure 3e. Composite control torque

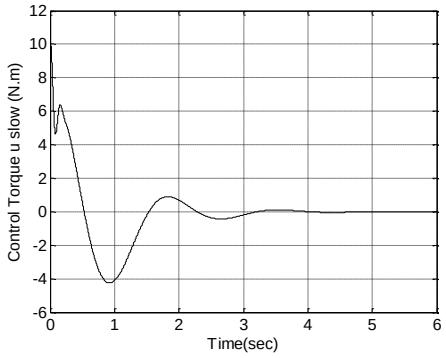

Figure 3f. Slow control torque

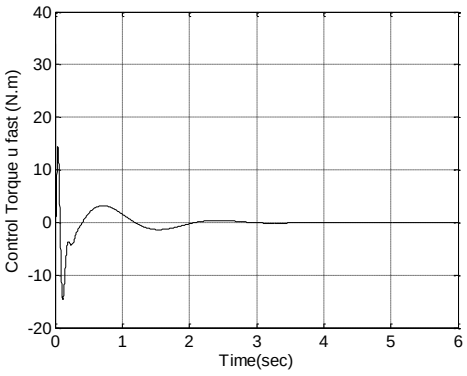

Figure 3g. Fast control torque

6 EXPERIMENTAL FLEXIBLE MANIPULATOR SYSTEM

This section describes the experimental flexible manipulator used in this study. Figure 4 shows a schematic diagram of the experimental rig, which consists of three main components: a flexible arm, the driving motor, measuring devices and a digital processor. The flexible arm is constructed using a piece of thin stainless-steel. The manipulator can be considered as a fixed-free flexible arm, which can bend freely in the horizontal plane but is relatively stiff in vertical bending and torsion. The rig equipped with a motor at the hub, driving the flexible manipulator. The motor is chosen as the drive

actuator due to its low inertia and inductance and physical structure.

The measuring devices used to record various responses are the shaft encoder and strain gauge. The shaft encoder, with a resolution of 400 pulses, is used to measure the hub angle. The strain gauge is attached near the hub as shown in Figure 4a to measure the fist mode oscillations which correspond to the first modal variable. There was no payload at the tip of the manipulator.

The processor is compatible with a data-acquisition card (DAQ) with a conversion speed of 50μs either for acquiring or generating signals; while programmable automation controller (PAC) is an advanced embedded control and it combines an embedded real-time processor, a high-performance FPGA, and swappable I/O modules. Each I/O module is connected directly to the FPGA, providing low-level customization of timing and I/O signal processing with a conversion speed of 5ns. The FPGA is connected to the embedded real-time processor via a high-speed PCI bus.

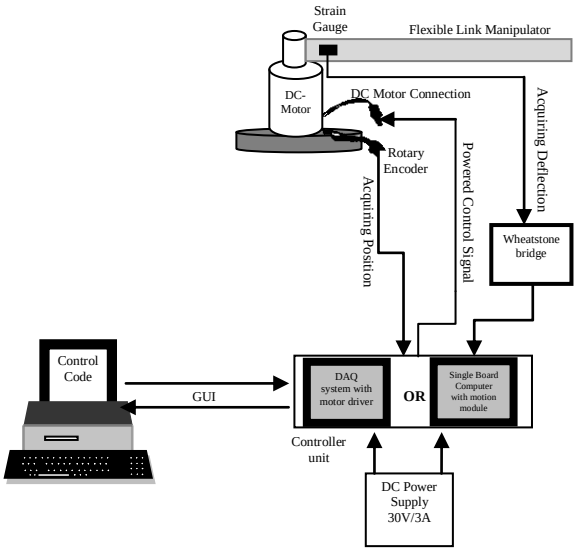

Figure 4a. Experimental rig

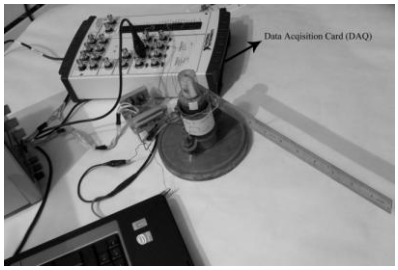

Figure 4b. The setup of FLM using DAQ architecture

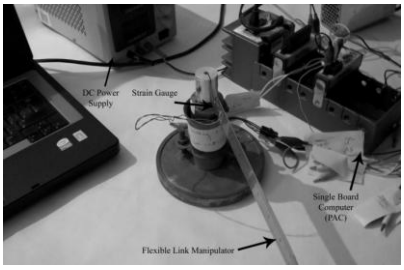

Figure 4c. The setup of FLM using PAC architecture

7 EXPERIMENTATIONS AND RESULTS

The proposed control strategy will be now studied by a series of experiments. Experimental investigations are carried out to demonstrate the effectiveness of the proposed method on the two different architectures.

7.1 Using DAQ system

The block diagram shown in Figure 5 presents the hardware implementation of the singular perturbation approach using a pulse width modulated (PWM) signal proportional to the desired torque. Increasing the PWM duty cycle results in increased torque.

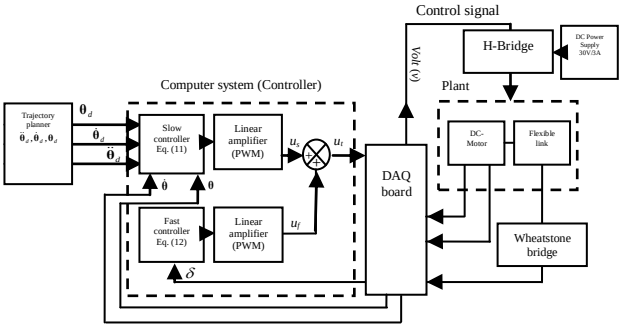

Figure 5. DAQ architectures model

Figure 6 shows I/O execution for control algorithm using DAQ system. Signals will be either generated from the computer to drive the motor or acquired from the optical encoder where the period of operation for each process is 50μs for the given DAQ board. On the other hand, the quadrature optical encoder will change its reading in 15ns in the worst case scenario according to its type.

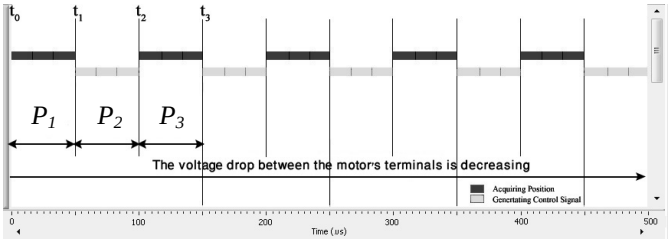

Figure 6. Input/Output tracing execution using DAQ

During the first period (t_0-t_1), angular position is being acquired while the motor is set to be running initially at full speed (100% duty cycle). During the second period (t_1-t_2) the DAQ is generating control signal (with a corresponding duty cycle) that matches the final acquired position in the first period. During this period the change in angular position of the motor is not felt by DAQ. This means that the control signal does not match the current actual position. During the third period (t_2-t_3), the DAQ starts acquiring position and thus the position value in the computer (controller) is being incremented. During that same period, the motor is still rotating under its own inertia. The fourth period will start by generating a control signal corresponding to the last acquired position and thus the duty cycle generated will be higher than what it is expected to be. Following this sequence, a steady-state error in the link position was expected to be of higher

value than desired. However, the actual generated control signal at the last several time periods was not strong enough to drive the motor. Hence, a steady-state error existed as shown in Figure 7a which is below the desired value. On the other hand, the link vibrations have been totally damped out after 0.8 seconds as shown in Figure 7b.

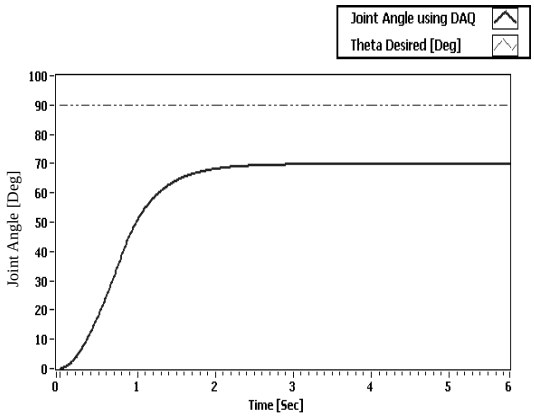

Figure 7a. Joint angle using DAQ before using model-reference algorithm

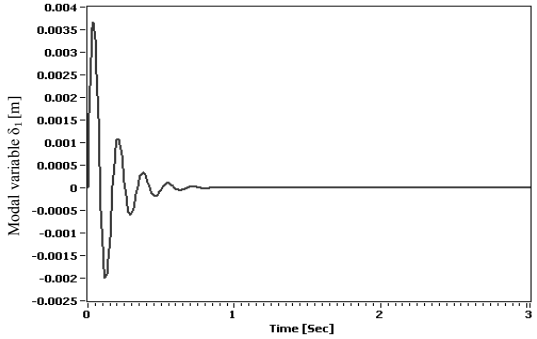

Figure 7b. First modal variable δ_1 using DAQ

7.2 Using PAC system

As mentioned before, the execution time using PAC is only 5 ns. Figure 8 shows the sequence of operation. During the first period (t_0-t_1), the PAC is acquiring the angular position of the motor, while the motor is initially set to be running at full speed. During the second period (t_1-t_2), PAC is generating a control signal corresponding to the previous sensor reading. Now at t_2 the time spent during the execution is 10ns that means the optical encoder didn't change its reading yet. Then from (t_2-t_3), PAC will acquire the new angular position. At t_3 the time is equal to 15ns the new reading for the angular position should have already been acquired and that reading will not change until another 15ns which will be reach at t_6. The control signal will be generated within (t_3-t_4) to match that change in position. This means that the PAC will match any kind of change through the optical encoder based on its high sampling rate. Figure 9a presents the step response for the link position showing no steady-state error. Figure 9b shows that the link vibrations have been totally damped out after 0.4 seconds which is almost half of that using DAQ system using the same control algorithm.

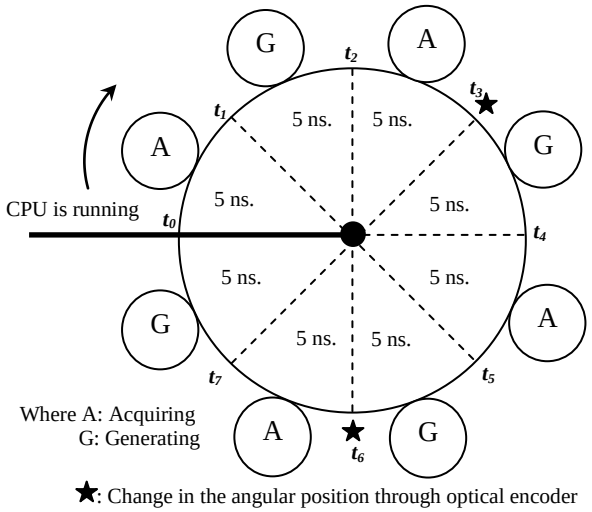

Figure 8. Scheduling process using PAC to control flexible link

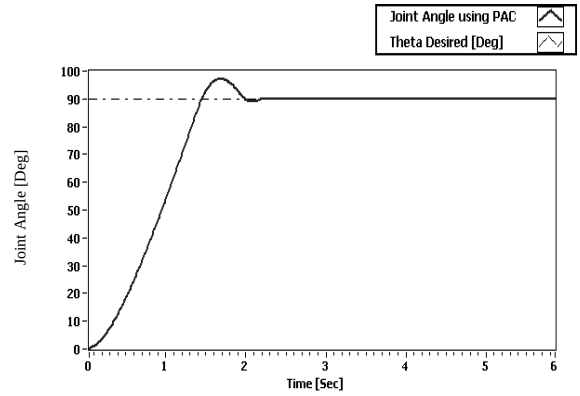

Figure 9a. Joint angle using PAC

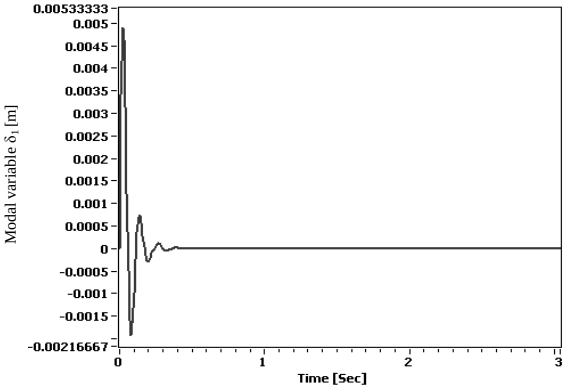

Figure 9b. First modal variable δ_1 using PAC

8 MODEL REFERENCE COMOSITE CONTROL ALGORITHM

To improve the response of the available DAQ system, a model-reference technique is introduced for vibration control of a flexible manipulator. Figure 10 presents the experimental setup. In this setup, the theoretical model is running on the same PC that generates the control signal based on the real-life measurements. The torque determined form the

theoretical model is converted into desired current ($i_{desired}$) by dividing it by the motor constant (k_t). The voltage determined from the control law is also converted into actual current (i_{actual}) through the motor transfer function (TF). The error between the desired and actual current signals (i_e) is then changed into voltage again through the motor TF and then multiplied by a proportional gain. This voltage signal becomes the input to the motor driver.

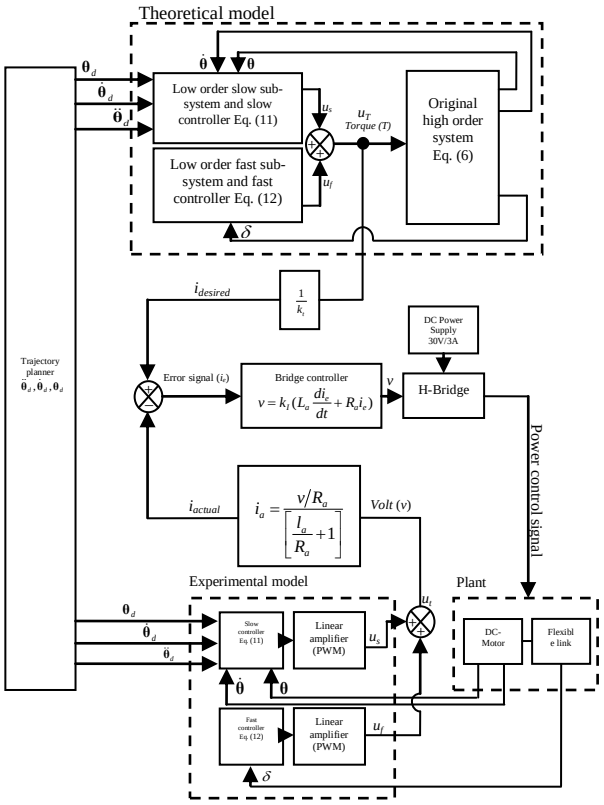

Figure 10. Experimental model-reference algorithm to implement the composite control strategy through (DAQ system)

Figure 11a shows the link position after using the model-reference composite control. It is clear that the steady-state error that existed in figure 7a is almost eliminated only after applying proportional control on the current error signal. Figure 11b shows that the link vibrations has been totally damped out after 0.6 seconds as shown.

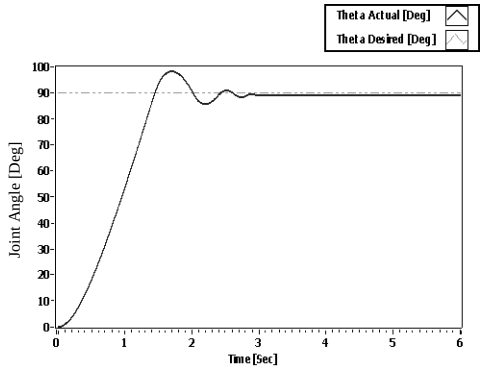

Figure 11a. Joint angle using after using model-reference algorithm

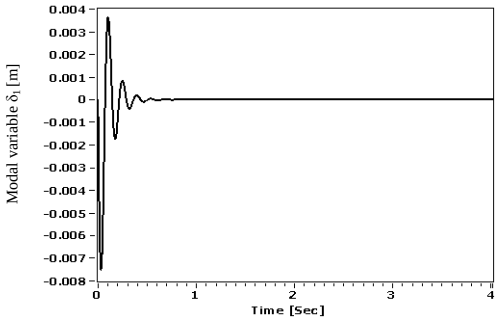

Figure 11b. First modal variable δ_1 after using model-reference algorithm

9 CONCLUSION

A singular perturbation approach has been utilized for the control of lightweight flexible-link manipulators. The main problem concerned with flexible-arm control, namely the number of the control inputs being less than the number of controlled variables, has been successfully faced by means of a model order reduction, which is a characteristic of a two-time-scale approach. Simulation results have shown the success of the approach. Experiments have been implemented for a flexible-arm prototype using two different hardware architectures in order to validate the results obtained in simulations. A low sampling rate device like (DAQ system) combined with a model-reference control strategy has proved to be sufficient to improve the dynamic performance of the actuator and hence shift the link end position to the desired location similar to a more expensive programmable automation controller.

APPENDIX A

The fixed-free deflection modes are [19]:

$$\phi_j(x) = (\sin\frac{a_j x}{L} - \sinh\frac{a_j x}{L}) - \frac{(\sin a_j + \sinh a_j)}{(\cos a_j + \cosh a_j)}(\cos\frac{a_j x}{L} - \cosh\frac{a_j x}{L}) \quad (A.1)$$

For $j = 1, 2$, $a_1 = 1.875$ and $a_2 = 4.694$.
The Lagrangian dynamic equations (2) result in:

$$M(\delta) = \begin{bmatrix} M_{11} & M_{12} & M_{13} \\ M_{21} & M_{22} & M_{23} \\ M_{31} & M_{32} & M_{33} \end{bmatrix} \quad (A.2)$$

where the elements of the previous equation are given as:

$$M_{11} = J_0 + M_p L^2 + I_0 + M_p(\phi_{1e}^2\delta_1^2 + 2\phi_{1e}\phi_{2e}\delta_1\delta_2 + \phi_{2e}^2\delta_2^2) \quad (A.3.a)$$

$$M_{12} = M_p\phi_{1e} + w_1 \quad \text{(A.3.b)}$$

$$M_{13} = M_p\phi_{2e} + w_2 \quad \text{(A.3.c)}$$

$$M_{21} = M_p\phi_{1e} + w_1 \quad \text{(A.3.d)}$$

$$M_{22} = m + M_p\phi_{1e}^2 + J_p\phi_{1e}'^2 \quad \text{(A.3.e)}$$

$$M_{23} = M_p\phi_{1e}\phi_{2e} + J_p\phi_{1e}'\phi_{2e}' \quad \text{(A.3.f)}$$

$$M_{31} = M_p\phi_{2e} + w_2 \quad \text{(A.3.g)}$$

$$M_{32} = M_p\phi_{1e}\phi_{2e} + J_p\phi_{1e}'\phi_{2e}' \quad \text{(A.3.h)}$$

$$M_{33} = m + M_p\phi_{2e}^2 + J_p\phi_{2e}'^2 \quad \text{(A.3.i)}$$

$$g_1 = 2M_p\dot{\theta}[(\phi_{1e}^2\delta_1 + \phi_{1e}\phi_{2e}\delta_2)\dot{\delta}_1 + (\phi_{1e}\phi_{2e}\delta_1 + \phi_{2e}^2\delta_2)\dot{\delta}_2] \quad \text{(A.4.a)}$$

$$g_{21} = -M_p\dot{\theta}^2[\phi_{1e}^2\delta_1 + \phi_{1e}\phi_{2e}\delta_2] \quad \text{(A.4.b)}$$

$$g_{22} = -M_p\dot{\theta}^2[\phi_{1e}\phi_{2e}\delta_1 + \phi_{2e}^2\delta_2] \quad \text{(A.4.c)}$$

$$K = \begin{bmatrix} k_{1e} & 0 \\ 0 & k_{2e} \end{bmatrix} \quad \text{(A.5)}$$

where

$$\phi_{ije} = \phi_{ij}(x)\Big|_{x=L},\ j = 1,2 \quad \text{(A.6.a)}$$

$$\phi_{ije}' = \left.\frac{d\phi_j(x)}{dx}\right|_{x=L},\quad j = 1,2 \quad \text{(A.6.b)}$$

$$w_j = \rho AL^2\int_0^1 \phi_j(x)x\,dx,\ j = 1,2 \quad \text{(A.6.c)}$$

$$k_{je} = \frac{EI}{L^3}\int_0^1\left[\frac{d^2\phi_j(x)}{dx^2}\right]^2 dx\ \ j = 1,2 \quad \text{(A.6.d)}$$

and *e* implies the end-effector.

REFERENCES

[1] W. J. Book, structure flexibility of motion systems in the space environment, IEEE Transactions on Robotics and Automation, Vol. 19, pp.524-530. 1993.

[2] W. J. Book, controlled motion in an elastic world, Tans. ASME, J. Dynamic Systems, Measurement, Control, Vol. 115, pp.253-261, 1993.

[3] R. H. Canon, E. Schmitz, initial experiments on the endpoint control of a flexible one-link robot, Int. J. Robot. Res., Vol. 3, No. 3, pp. 62-75, 1984.

[4] C. Menq, and J. Z. Xia, experiments on the tracking control of a flexible one-link manipulator, ASME J. Dyn. Syst. Meas. Control, Vol. 115, pp. 306-308, 1993.

[5] S. R. Kuldip, V. Feliu and H. B. Benjamin, identification and control of a single-link flexible manipulator, in: Proc. Conf. on Decision and Control, Austin, TX, pp. 2278-2280, 1980.

[6] M. W. Spong, modeling and control of elastic joint robots, J. Dyn. Syst. Measurement Control, Vol. 109, pp. 310-319, 1987.

[7] Y. P. Chen, regulation and vibration control of a FEM-based single-link flexible arm using sliding-mode theory, J. Vib. Control, Vol. 7, No. 5,pp. 741-752, 2001.

[8] Z. Su, and K. Khorasani, a neural-network-based controller for a single-link flexible manipulator using the inverse dynamics approach, IEEE Trans. Ind. Electron., Vol. 48, No. 6, pp. 1074-1086,2001.

[9] Y. F. Lu, Z. X. Shi, G. M. Feng, and Y. X. Han, gauge principle formulation and adaptive control and tracking of the flexible manipulator, Proceedings of the ASME Dynamic System and Control Division, Vol. 57, No. 1 pp.179-184, 1995.

[10] S. Rai, and H. Asada, integrated structure control design of high speed flexible robots based on time optimal control, J. Dyn. Syst. Meas. Control, Vol. 117, pp. 503-512, 1995.

[11] K. Yoshida, T. Shimogo, and K. Murano, digital optimal control of elastic structure systems, JSME Int. J., Vol. 30, pp. 1311-1318, 1987.

[12] E. H. Fung, and F. C. Cheung, variable structure tracking controller for a flexible one-link robot, Proceedings of IEEE International Conferences On System, Man Cybernetics, Vol. 5,pp. 4458-4463, 1995.

[13] H. G. Lee, S. Arimoto and F. Miyazaki, Liapunov stability analysis for PDS control of flexible multi-link manipulators, in: Proc. Conf. on Decision and Control, Austin, TX, pp. 75-80, 1988.

[14] F. Mastsuno, and A. Hayashi, PDS cooperative control of two one-link flexible arms, in: Proc. IEEE Int. Conf. on Robotics and Automation, San Francisco, CA, pp. 1490-1495, 2000.

[15] B. Siciliano, W. J. Book, a singular perturbation approach to control of lightweight flexible manipulators, The International Journal of Robotics Research, Vol. 7, No. 4, pp.79-90, 1988.

[16] P. V. Kokotovic, applications of singular perturbation techniques to control problems, SIAM Review. Vol. 24, No. 4, pp. 501-550, 1984.

[17] A. H. Nayfeh, introduction to perturbation techniques, Willey, New York, 1993.

[18] A. Bensosman, and G. Le Vey, control of flexible manipulators: a survey, Robotica, Vol. 22, No. 5, pp. 533-545, 2004.

[19] L. Meirovitch, fundamentals of vibrations, McGraw Hill, 2001.

[20] P. V. Kokotovic, H. K. Khalil and J. O'Reilly, singular perturbation in control, SIAM, 1999.

[21] K. Ogata, modern control engineering, 5th ed., Pearson, 2010.

[22] J. D. Hoffman, numerical methods for engineers and scientists, McGraw-Hill, New York, 2001.